How changes in future precipitation impact flood frequencies: a quantilequantile mapping approach

Water Resources Research

RESEARCH ARTICLE
10.1029/2024WR038471

How Changes in Future Precipitation Impact Flood Frequencies: A Quantile-Quantile Mapping Approach

Luigi Cafiero[1], **Miriam Bertola**[2], **Paola Mazzoglio**[1], **Günter Blöschl**[2], **Francesco Laio**[1], **and Alberto Viglione**[1]

[1]Dipartimento di Ingegneria dell'Ambiente, del Territorio e delle Infrastrutture, Politecnico di Torino, Turin, Italy, [2]Institute of Hydraulic Engineering and Water Resources Management, Vienna University of Technology, Vienna, Austria

Key Points:

- An operative procedure to include the expected change in precipitation extremes into flood frequency analysis through q-q plots is proposed
- The assumptions of the method are tested through a simulation study using a simple rainfall-runoff model
- The procedure is applied to a case study in the Po River basin to project future changes of the 100-year return period floods

Correspondence to:
L. Cafiero,
luigi.cafiero@polito.it

Citation:
Cafiero, L., Bertola, M., Mazzoglio, P., Blöschl, G., Laio, F., & Viglione, A. (2025). How changes in future precipitation impact flood frequencies: A quantile-quantile mapping approach. *Water Resources Research*, *61*, e2024WR038471. https://doi.org/10.1029/2024WR038471

Received 2 DEC 2024
Accepted 15 JUN 2025

Author Contributions:
Conceptualization: Luigi Cafiero, Francesco Laio, Alberto Viglione
Data curation: Luigi Cafiero, Miriam Bertola, Paola Mazzoglio
Formal analysis: Luigi Cafiero
Investigation: Luigi Cafiero
Methodology: Luigi Cafiero, Miriam Bertola, Günter Blöschl, Francesco Laio, Alberto Viglione
Software: Luigi Cafiero
Supervision: Alberto Viglione
Validation: Luigi Cafiero, Alberto Viglione
Visualization: Luigi Cafiero
Writing – original draft: Luigi Cafiero
Writing – review & editing: Miriam Bertola, Paola Mazzoglio, Günter Blöschl, Alberto Viglione

Abstract Flood risk management institutions and practitioners need reliable and easy-to-use approaches that incorporate the changing climate conditions into flood predictions in ungauged basins. The present work aims at developing an operative procedure to include the expected variation in precipitation extremes in flood frequency analysis. We relate Flood Frequency Curves (FFC) and Intensity-Duration-Frequency curves through quantile-quantile relationships, whose slopes represent the elasticity of floods to precipitation extremes. Assuming that the percentage variations of precipitation and flood quantiles are linked by the quantile-quantile relationship, we obtain modified FFC accounting for the projected changes in precipitation extremes. The methodology is validated in a virtual world inspired by the Rational Formula approach, where flood events are the result of the combination of two jointly distributed random variables: extreme precipitation and peak runoff coefficient. The proposed methodology is found to be reliable for large return periods in basins where flood changes are dominated by precipitation changes rather than variations in the runoff generation process. To illustrate its practical usefulness, the procedure is applied to 227 catchments within the Po River basin in Italy using projected percentage changes of precipitation extremes from CMIP5 CORDEX simulations for the end of the century (2071–2100) and RCP 8.5 scenario. With projected changes in 100-year precipitation ranging from 5% to 50%, the corresponding variations in 100-year flood magnitudes are expected to span a broader range (10%–90%). A substantial heterogeneity in catchment responses to rainfall changes exists due to different elasticities of floods to precipitation extremes.

Plain Language Summary Flood risk managers need tools that are both reliable and easy to use to account for climate change when predicting floods in areas without measurement stations. This study develops a practical method to account for changes in extreme rainfall in flood predictions. The method is based on relating the probability distributions of floods and of extreme rainfall, which can be estimated by common applied hydrology methods, through q-q plots, that is, graphical methods to compare statistical models. By assuming invariance of the q-q plot slope in time, changes in flood frequency can be derived from expected increases in extreme rainfall. We demonstrate that the method works well for large floods and where changes in soil moisture, land-use and river training are less relevant than extreme rainfall changes. By applying this method in the Po River basin in Italy, using future rainfall projections from climate models, the predicted increases in severe floods range from 10% to 90%.

1. Introduction

The alteration of climate patterns significantly impacts the hydrology of river basins, resulting in significant implications for water resource management and infrastructure planning (Bloetscher, 2012; Dong et al., 2020). Specifically, Gobiet et al. (2014) found that the Alpine region is expected to experience an increase in the intensity of extreme precipitation events in all seasons and for most regions, leading to an increased potential for extreme flooding (Wilhelm et al., 2022). As the urgency of climate change adaptation measures becomes more evident, public administrations are recognizing the critical need to incorporate its effect on hydrological risk, in order to ensure that their infrastructures are resilient in the face of changing environmental conditions. The EU Floods Directive (2007/60/EC) states that consideration should be given to the expected impacts of climate change on flood occurrence. However, a standardized methodology for this purpose is not available at present (European Commission, 2021). It is therefore of interest to quantify the effect of climate change, and in particular of the increase of extreme precipitation, on Flood Frequency Curves (FFC), which are used in the field of hydrological

engineering to assess flood hazards and design hydraulic structures. FFCs provide the probability of exceeding a given flow rate within a specified time interval and are traditionally based on the assumption of stationarity in time.

Hall et al. (2014) provide an assessment of the most widespread methods to detect and analyze flood changes. They identify three main groups of potential drivers of change: (a) river channel engineering and hydraulic structures, (b) land use change and (c) climatic change, which have different impacts according to the spatial scale of interest (Blöschl et al., 2007; Viglione et al., 2016). Two main strategies exist for gaining knowledge on flood regime changes. The first is the data-based approach which requires long and reliable data series, and does not need knowledge of the physical principles leading to those changes. In this regard, the Mann-Kendall test or the Pettitt test are widely applied in literature (Villarini et al., 2011), as well as the Chi-square test on parametric Poisson regression (Mangini et al., 2018), to detect gradual or step changes in the mean flood. The second is the process-based approach in which cause-effect relationships are used to represent the chain of processes from climate over catchment to the river network (Hall et al., 2014). Where long and reliable data series are not available, or are missing as in ungauged basins, the process-based approach is the most used prediction tool. In this regard, Barbhuiya et al. (2023) provide a review of the methods developed to deal with non-stationarity in flood frequency analysis, including some case studies. The most popular approach, which is a combination of data-based and process-based methods, is the use of time-varying parameters of the probability distribution of flood peaks, using time or hydroclimatic variables like temperature or mean annual precipitation as covariates. Generalized Additive Models are used to estimate the location, shape and scale parameters of the distribution (GAMLSS framework). For example, Šraj et al. (2016) compared stationary and non-stationary models using the GEV distribution with parameters dependent on time and annual precipitation. They found that the best performance for 2 gauging stations in Slovenia is obtained using the annual precipitation as a covariate. Westra et al. (2013) used globally averaged near-surface temperature as a covariate for non-stationary generalized extreme value analysis, finding a statistically significant association with precipitation extremes at the global scale. A similar approach was developed by Anzolin et al. (2023) who considered climatic drivers of floods as covariates, to improve non-stationary flood frequency analysis in Brazil. They assumed a linear dependency between the location parameter of a GEV distribution and the selected covariates. Their results suggest that using local climate information (annual rainfall and annual maximum rainfall), or global climate information (El Niño Southern Oscillation) as covariates leads to better model performance when there is a significant correlation between flood and climate covariates. However, such kind of approaches may not be suitable for small-scale analyses, where local phenomena may blur large-scale atmospheric factor (Steirou et al., 2019). Moreover, short-term trends and multi-decadal shifts in some hydrological variables may be a limitation to this kind of approach (Koutsoyiannis & Montanari, 2015).

Another approach to deal with non-stationarity in gauged and ungauged basins is the regional flood frequency analysis, which allows to improve flood quantile estimation by pooling information from multiple sites according to geographical or hydrological similarity (Vogel et al., 2011). For example, Bertola et al. (2020) estimated regional flood trends using a regional Gumbel distribution, whose median and growth factor can change in time with different strengths for different catchment sizes. Their analysis revealed distinct trends across different European regions. Additionally, Bertola et al. (2021) proposed a framework for attributing these flood changes to potential drivers. In southern Europe, both antecedent soil moisture and extreme precipitation contribute to flood changes, and their relative importance depends on the return period. Cunderlik and Burn (2003) used a different approach, separating the non-stationary pooled quantile function into a time-dependent local component and a time-independent regional component. Leclerc and Ouarda (2007) introduced a regional Flood Frequency Analysis at ungauged sites using a multiple regression model with 2–4 explanatory variables within the hydrologic neighborhood. Other strategies to include non-stationarity imply the usage of Bayesian approaches to incorporate expert knowledge into the modeling process (Barbhuiya et al., 2023). In particular, Guo et al. (2022) proved that non-stationary Bayesian regional flood frequency analysis coupled with linear mixed effect reduced flood estimation uncertainty when compared to stationary generalized least squares model in the Dongting Lake basin (China). A different approach was developed by Fiseha et al. (2014) and Mishra and Herath (2015) who used regional climate models to assess the hydrological responses to climate change in the Upper Tiber River basin (Central Italy) and in the Bagmati River (Nepal). They used a physically based model which was first calibrated with observed data and then forced with bias-corrected daily regional climate model outputs. Although effective, this method demands meticulous calibration and complex bias correction, making it less practical for broad implementation across multiple catchments.

A standardized operational method for incorporating non-stationarity in the calculation of the FFCs is still lacking. In this paper, we introduce a pragmatic but reliable approach for modifying FFCs to accommodate the shift in precipitation extremes derived from climate model projections, which only requires the FFC and the Intensity-Duration-Frequency (IDF) curves of a generic basin. We adopt the methodology proposed by Breinl et al. (2021), who compared IDF curves of maximum annual rainfall with FFCs while introducing the concept of elasticity as an indicator of the sensitivity of floods to changes in precipitation extremes. We define quantile-quantile (q-q) relationships between FFC and IDF curves, and we assume that their logarithmic slope, or elasticity, can be used to transform the percentage variation of precipitation quantiles into percentage change of flood quantiles. This hypothesis is the core of the present work and is analyzed in the paper. In particular, the paper investigates the following three research questions, two methodological and a case-specific one:

1. In which conditions are we allowed to use the methodology? i.e., in which conditions does the hypothesis of using the slope of the q-q relationships for flood change projection hold?
2. Is this methodology suitable across the full distribution of floods? i.e., for all return periods?
3. What are the expected flood changes for projected precipitation changes in Northern Italy?

The paper is structured as follows: in Section 2 we provide a description of the methodology, in Section 3 we analyze the validity of the hypothesis of usability of the q-q relationship to derive changes in the FFC underlying the study, and in Section 4, in order to illustrate the application of the method to real data, we present the case study in the Po River basin in Northern Italy. The paper ends with a discussion section and conclusions.

2. Methodology: q-q Relationship and Simple Hydrological Model

Consider a precipitation event hitting a catchment and generating a flood peak at the outlet. We call P the average liquid precipitation intensity over the catchment, and Q the corresponding peak discharge at the outlet, normalized by the catchment area in order to have the same units (e.g., mm/hr) for both P and Q. The rainfall intensity P is supposed to be averaged in space and time: in space, over the catchment area (or the contributing area when rainfall falls in liquid form only in a portion of the basin); in time, over the so-called critical duration, that is the duration maximizing the peak discharge for that given catchment. Notice that, in practice, the selection of the correct rainfall duration is not key to application we are proposing here (more details on this point will be discussed later, after having set the basis for our reasoning in the following paragraphs). Under the mentioned definitions, the relation between Q and P can be formalized as

$$Q = C \cdot P \tag{1}$$

where C is the peak runoff coefficient (non-dimensional, $0 \leq C \leq 1$). At the event scale, C and P are both random variables, with a potential mutual dependence since antecedent moisture conditions are often positively correlated: more intense rainfall events often come in clusters or with duration larger than the critical one for the catchment, potentially wetting the soil before the start of the peak-runoff generation phase. Let F_Q be the cumulative distribution function of annual floods, and F_P the cumulative distribution function of max annual precipitation for the critical duration of the catchment, obtained independently. When accompanied by the indices 0 or 1, they refer specifically to the probability distributions in the reference period (0) or future period (1). Suppose the current-climate probability distribution of extreme rainfall, F_{P_0}, and peak discharge, F_{Q_0}, are known for the given catchment. Also suppose climate projections are available, under different scenarios, enabling one to estimate the expected future probability distribution of extreme rainfall, F_{P_1}, or, equivalently, the future extreme rainfall quantiles for given probability level, q_{P_1}, possibly expressed in variation terms with respect to the current values, $q_{P_1} = q_{P_0}(1 + \delta)$, with δ being the expected future variation. Under these very common conditions, it is often asked by the stakeholders to estimate the expected future probability distribution F_{Q_1} or quantiles q_{Q_1} of peak discharges. In the following, we develop an operational method to provide these estimates. We estimate the temporal variations of the flood frequency curve from projected changes in the frequency curve of rainfall using the logarithmic slope of the quantile-quantile (q-q) relationship. This relationship is defined by combining the flood and rainfall frequency curves. Given a value y of rainfall for the catchment's critical duration, the q-q relationship that relates y to the value z of the flood peak with the same non-exceedance probability is described in Equation 2 and considered stationary in time.

$$z = F_{Q_0}^{-1}(F_{P_0}(y)) = F_{Q_1}^{-1}(F_{P_1}(y)) \tag{2}$$

This assumption will be thoroughly analyzed in the following sections. We obtain the modified flood frequency curve F_{Q_1} according to the variation of the frequency curve of rainfall:

$$F_{Q_1}(z) = F_{Q_0}\left(F_{P_0}^{-1}(F_{P_1}(y))\right) \tag{3}$$

where the lower apex "0" and "1" stand for a present and a future period respectively. Please note that the purpose here is to recreate what is generally available in operative conditions: the probability distributions of flood and precipitation are indeed obtained independently and the quantiles do not correspond to the same events. To validate the hypothesis underlying Equations 2 and 3, we set up a simple model based on the rational method, where flood events Q are the result of the combination of two jointly distributed random variables: the maximum annual rainfall for the time of concentration of the catchment P and the peak runoff coefficient C, as in Equation 1 (Mulvaney, 1850). We assume that the probability distribution of the precipitation F_P is a Gumbel distribution, the probability distribution of the peak runoff coefficient F_C is a beta distribution (Gottschalk & Weingartner, 1998; Merz et al., 2006; Viglione et al., 2009). C and P are correlated through a Gumbel copula, so that

$$F_{C|P}(x|y) = \mathbb{P}(U < u|V = v) = \frac{\partial}{\partial v}C_\theta(u,v) = \frac{C_\theta(u,v)}{v}\left[(-\ln u)^\theta + (-\ln v)^\theta\right]^{-1+1/\theta}(-\ln v)^{\theta-1} \tag{4}$$

where $u = F_C(x;\alpha,\beta) = I_x(\alpha,\beta)$ is the beta distribution of C with parameters α and β (expressed through the regularized incomplete beta function),

$$F_P(y;\xi,\sigma) = \exp\left(-\exp\left(-\frac{y-\xi}{\sigma}\right)\right) \tag{5}$$

is the Gumbel distribution of P with location parameter ξ and scale parameter σ, and

$$C_\theta(u,v) = \exp\left[-\left((-\ln u)^\theta + (-\ln v)^\theta\right)^{1/\theta}\right] \tag{6}$$

is the bivariate Gumbel Copula which attributes an increasing correlation between the two random variables as the rainfall amount increases. In the equations, ";" separates random variables from parameters, and "|" separates a variable to variables upon which it is conditional. The virtual world here simulated is obtained by generating one event per year for both precipitation and flood (i.e., the annual maxima of Q and P correspond to the same event). Generating more than one event per year, and therefore allowing the annual maximum P and Q not to be the same event, does not significantly change the results of the analysis (and therefore it is not shown in this paper). This framework is in agreement with the results of Fiorentino et al. (2007), who compared cumulated rainfall and relative flood peaks using a distributed hydrological model. They found that for lower values of rainfall, flood peaks have more dispersion compared to more intense events because the initial conditions of the soil are more variable. The choice of the copula family is not part of the subsequent sensitivity analysis; however, similar results were obtained considering a Gaussian copula instead. We assume that the distribution of C conditional on P does not change for the different climatic conditions, which is consistent with the assumption that the hydrologic response of the catchment does not change in time. This assumption is commonly employed in process-based methods for climate change impact assessment in hydrology. Similarly to Viglione et al. (2009), but assuming that C and P are dependent, the CDF of flood, product of the two, is calculated as

$$F_Q(z;\alpha,\beta,\xi,\sigma) = \int_\Omega F_{C|P}\left(\frac{z}{y}|y;\alpha,\beta\right)\cdot f_P(y;\xi,\sigma)dy \tag{7}$$

where Ω indicates all possible values of P.

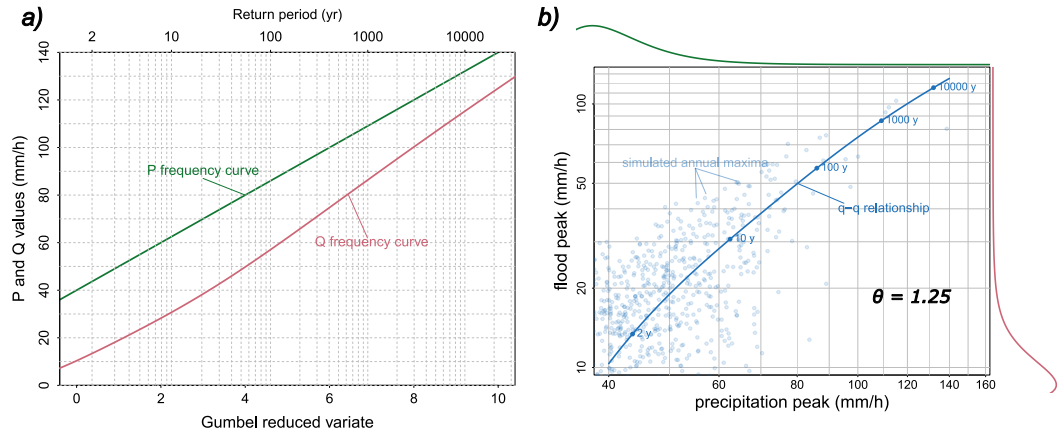

Figure 1. (a) Frequency curve of flood peaks and rainfall maxima for a hypothetical catchment obtained with the model based on the rational method (Equations 1 and 4–7) with $\alpha_0 = 2, \beta_0 = 4, \xi_0 = 40$ mm/hr, $\sigma_0 = 10$ mm/hr. The random variables P (rainfall) and C (peak runoff coefficient) are slightly correlated ($\theta = 1.25$). (b) Quantile-quantile relationship (blue line) obtained from the frequency curves on the left with the pairs of annual maxima of rainfall and flood (dots). The curves on the top and on the right of panel (b) are proportional to the probability density functions of P and Q respectively. Note that the axes have been limited to emphasize the behavior of larger events.

Figure 1 shows one hypothetical case, used as a reference case hereafter, where $\alpha_0 = 2, \beta_0 = 4, \xi_0 = 40$ mm/hr, $\sigma_0 = 10$ mm/hr, and the random variables P and C are slightly correlated ($\theta = 1.25$, which corresponds to Kendall correlation coefficient $\tau = 0.2$). In this way, the correlation between Q and P is similar to those found in real catchments in Austria (Blöschl et al., 2024). The frequency curves for rainfall and flood, along with the q-q relationship are shown, including $N = 1{,}000$ pairs of simulated annual maxima of P and Q.

3. Investigation on the Method's Main Assumption

The methodology proposed in this article relies on the assumption that the logarithmic slope of the q-q relationships, or elasticity E^{qq}, can be used to transform the percentage variation of rainfall quantiles (q_P) into percentage change of flood quantiles (q_Q)

$$\Delta q_Q = \Delta q_P \cdot E^{qq} \tag{8}$$

where

$$E^{qq} = \left.\frac{dq_Q}{dq_P}\right|_{q_P} \cdot \frac{q_P}{q_Q} \tag{9}$$

We investigate here the validity of Equation 3 using simulated variables according to Equations 4–7 when the parameters of the distributions change and considering different values of θ, that is different correlations between the random variables P and C. Suppose we have an hypothetical catchment characterized by a present climate with rainfall distribution parameters $\xi_0 = 40$ mm/hr and $\sigma_0 = 10$ mm/hr, and a future climate with $\xi_1 = 44$ mm/hr and $\sigma_1 = 11$ mm/hr. Additionally, suppose that the hypothetical catchment has a peak runoff coefficient with parameters $\alpha_0 = 2$ and $\beta_0 = 4$ which does not change in time ($\alpha_1 = 2$ and $\beta_1 = 4$). Figure 2 shows the correspondent q-q relationships of the reference and future periods, as well as the shift of some of the quantiles (black lines). In other words, our hypothesis is that the elasticity of the reference q-q relationship (E^{qq}), available in operative conditions, approximates the elasticity of the lines describing the shift of the equi-quantiles points from reference to future period (E^{ref}). In practice, for each quantile, we track the shift from the reference to the future along the quantile axis. This allows to construct a continuous representation of how the distribution evolves. By calculating the logarithmic slope of this shift at each quantile, we capture the rate of change in the distribution at that specific point. The resulting curve of these slopes provides a detailed, continuous view of the differences between the reference and future distributions, reflecting how the entire

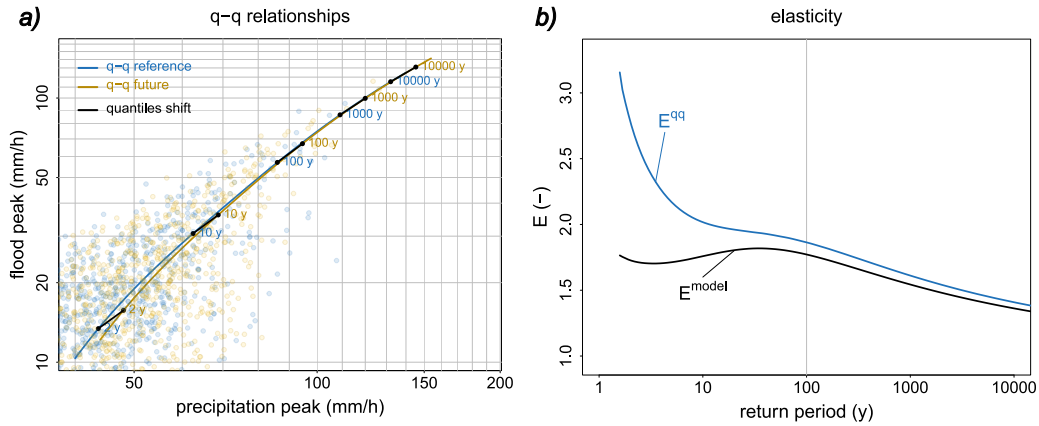

Figure 2. (a) q-q relationships obtained for the reference and the future periods. The colored dots represent pairs of simulated annual maxima of precipitation and flood. The two periods differ only in terms of rainfall distribution: both the location and scale parameters are increased by 10%. The response of the catchment in terms of flood generation mechanism is kept constant and modeled through a beta distribution, which describes the peak runoff coefficient. Black lines represent some examples of the quantiles shifting from the reference to the future period. (b) Elasticity comparison between the quantiles shifting (black) lines and the q-q relationship in the reference period (blue) as a function of return periods. In this specific case, the elasticities are similar for return periods larger than 20–30 years.

distribution has shifted and changed over time $\left(E^{\text{ref}}\right)$. In an operative context, E^{ref} is not available, while E^{qq} can be easily obtained from the frequency curves of rainfall and flood. In our ideal numerical simulation both the elasticities are available, and E^{ref} is used as a reference for E^{qq} to validate the methodology in Figure 2b. For small return periods the elasticity is overestimated but, starting from a return period of 20–30 years they become comparable. Given the imposed arbitrary variation of rainfall quantiles, future flood quantiles are obtained using the elasticities as a multiplicative factor.

$$\begin{aligned} q_{Q_1}^{\text{qq}} &= q_{Q_0} \cdot \left(1 + \Delta q_P \cdot E^{\text{qq}}\right) \\ q_{Q_1}^{\text{ref}} &= F_Q^{-1}\left(p, \alpha_0, \beta_0, \xi_1, \sigma_1, \theta_0\right) = q_{Q_0} \cdot \left(1 + \Delta q_P \cdot E^{\text{ref}}\right) \end{aligned} \tag{10}$$

where $q_{Q_1}^{\text{qq}}$ is the future flood quantile with probability level p obtained with the q-q approach, $q_{Q_1}^{\text{ref}}$ is the future flood quantile obtained with the model based on the rational method principles, q_{Q_0} is the flood quantile in the reference or present period, and Δq_P is the percentage variation of precipitation quantile. The validity of the proposed methodology is quantified through the percentage error PE of future flood quantiles obtained with the q-q approach with respect to those obtained from the model.

$$PE = \frac{q_{Q_1}^{\text{qq}} - q_{Q_1}^{\text{ref}}}{q_{Q_1}^{\text{ref}}} \cdot 100 \tag{11}$$

Results are shown in Figure 3 and prove that in this specific case, the methodology is reliable starting from return periods larger than 20 years. From now on, the focus will be on the 100-year return period flood ($p = 0.99$) as a representative example of large return periods.

The percentage error of the 100-year flood estimated for the future period PE_{100} depends on the parameters of q-q relationships of present $\left(\alpha_0, \beta_0, \xi_0, \sigma_0, \theta_0\right)$ and future period $\left(\alpha_1, \beta_1, \xi_1, \sigma_1, \theta_1\right)$. It is therefore relevant to investigate the sensitivity of the PE_{100} to these parameters to define optimal basin characteristics and rainfall variation for the applicability of the methodology. The parameters α and β describe the catchment characteristics in terms of its response to rainfall events: α indicates the "concentration" of probability toward larger values of peak runoff coefficient, while β indicates the "concentration" of probability toward lower values. The parameter θ describes the correlation between the annual maxima of flood and rainfall. Given the operational nature of the proposed methodology, these three parameters are considered to be stationary in time: $\alpha_0 = \alpha_1$, $\beta_0 = \beta_1$, and

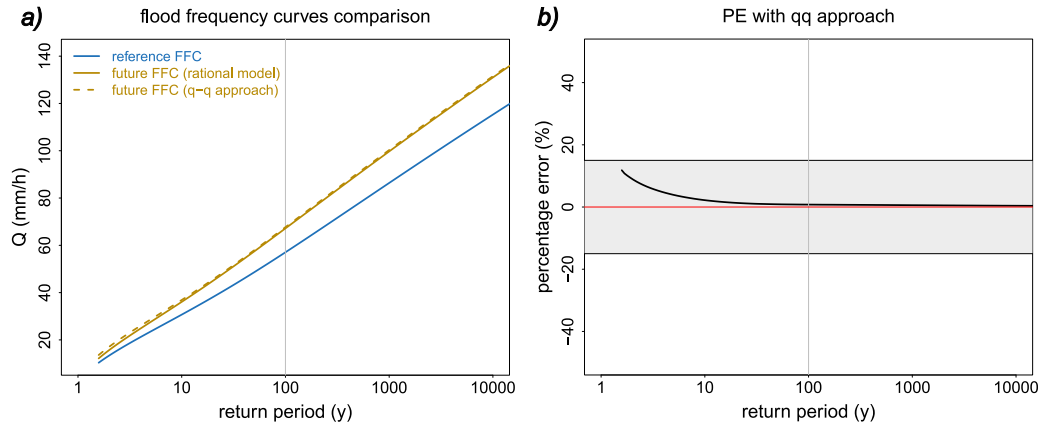

Figure 3. (a) Comparison of Flood Frequency Curves (FFC) obtained for the reference period (blue) and for the future period (yellow) considering the variation of rainfall distribution. Solid lines represent the FFC according to the model based on the rational method principle, while the dashed line represents the FFC according to the q-q approach. The difference tends to decrease with increasing return periods. (b) Percentage error of flood quantiles obtained for the future period using the q-q approach when compared to the flood quantiles of the future period obtained with the model based on the rational method principle. 15% error bounds are also shown. Note that the methodology is developed for large return periods (e.g., >100 years).

$\theta_0 = \theta_1$. Note that the marginal distribution of C is not stationary over time, whereas the conditional distribution of C given P is stationary. The sensitivity analysis is made on these parameters to investigate for which types of basins the q-q approach gives good results, as well as on the parameters ξ_1 and σ_1 describing the expected rainfall variation to investigate if the nature of rainfall variation has an impact on the validity of our hypothesis.

Nine types of catchments are identified in Figure 4 in terms of the type of response of the catchment and correlation between the annual maxima pair of flood and rainfall. In the first row and the last column, the different response types of the hypothetical catchments are described. In the second row of the figure, we analyze an arid (or high-infiltration) catchment in terms of peak runoff coefficient distribution modeled with $\alpha_0 = 1.2$ and $\beta_0 = 10$, in the third row the parameters of the peak runoff distribution are $\alpha_0 = 2$ and $\beta_0 = 4$ resulting in an intermediate catchment, and in the last row the parameters are $\alpha_0 = 3$ and $\beta_0 = 2$ resulting in a humid (or low-infiltration) catchment. The correlation between the random variables C and P increases from left to right. The first column is characterized by rainfall and peak runoff coefficient fully uncorrelated (note that rainfall and flood are instead correlated). The second column is modeled with a parameter $\theta_0 = 1.25$. The third column is obtained with peak runoff coefficient and rainfall almost fully correlated. In each image, the percentage error of the estimated 100-year flood PE_{100} for the future period obtained with the q-q approach for different scenarios of variation of rainfall distribution is presented. The x-axis of Figure 4 indicates an increase in terms of the location parameter ξ_1, that is, an increase in the mean of annual maxima, while the y-axis indicates an increase in terms of the scale parameter σ_1, that is, mainly an increase in the variance of annual maxima. The values of ξ_0, σ_0, ξ_1, and σ_1, are representative of the catchment sample available for the case study in Section 4 (see Appendix B). The sensitivity analysis indicates that the peak runoff coefficient distribution has minimal influence on the methodology's accuracy: generally, the methodology yields better results for humid catchments. Regarding the catchment characteristics, the correlation between rainfall and peak runoff coefficient, and hence between rainfall and flood, is relevant with results that become more accurate as the correlation increases. Finally, the nature of the rainfall distribution variation is also relevant: when the variation of precipitation extremes is in the mean (i.e., in the location parameter of the Gumbel distribution) the results are better than in the case where the variation of precipitation extremes is in their variability (i.e., in the scale parameter of the Gumbel distribution). This is particularly true for low values of correlation between flood and rainfall, and arid (or high-infiltration) basins.

4. Case Study

To illustrate its practical application, the methodology discussed above is applied to a case study set in the Po River basin in northern Italy. This area is characterized by a large alluvial plain surrounded on three sides by mountains. We analyze 227 catchments selected among those reported in Claps et al. (2024), with areas

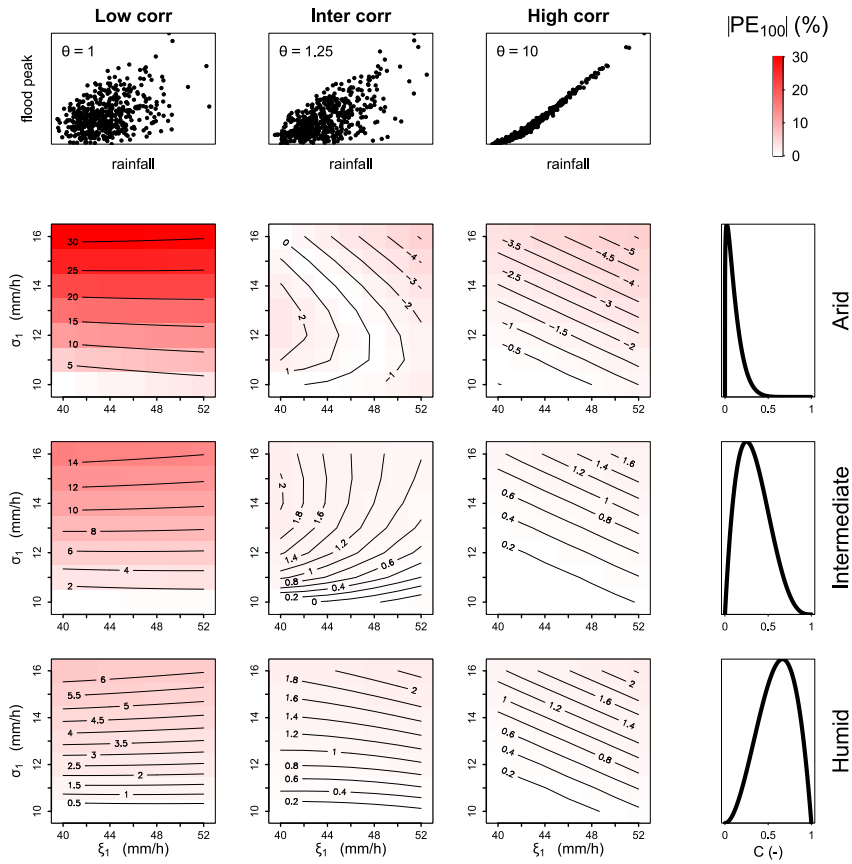

Figure 4. Sensitivity analysis of the percentage error of the 100-year flood obtained for the future period using the q-q approach when compared to the 100-year flood of the future period obtained with the model based on the rational method principle (Equation 11). Different types of catchments are analyzed in terms of aridity and correlation between flood and precipitation as schematized in the figures in the first row and the last column. In the second row the basins are assumed to be arid, in the third row intermediate, and in the last row they have a humid behavior. Along the different columns, the correlation between the pairs of peak runoff coefficients and precipitation annual maxima is increased. In the first column, there is no correlation; in the second column, the correlation is similar to a real case scenario, and in the third column, there is almost full correlation. The percentage errors for the 100-year flood are shown for different values of future precipitation distribution.

ranging from 10 km^2 to 13,700 km^2, and mean elevation from 161 to 3,123 m a.s.l. The selection was made according to the availability of at least 5 records of annual flood and areas smaller than 15,000 km^2. These criteria depend on the application of the regional Flood Frequency Analysis described in the specific section below. Basins strongly influenced by hydraulic structures or large reservoirs were also discarded. Figure 5 shows the location of the outlets of the 227 basins and the corresponding catchment boundaries. Considering all the 227 stations, the station-years available are 5637. The FFCs and the IDF curves for the maximum annual precipitation, which are needed to apply the non-stationary analysis through the quantile-quantile approach, are obtained independently through the regional procedures described below. This methodology can also be applied to ungauged catchments.

4.1. Intensity Duration Frequency Curves

Extreme rainfall measurements are obtained from the Improved Italian—Rainfall Extreme Data set or $I^2 - RED$ (Mazzoglio et al., 2020), a collection of short-duration (1, 3, 6, 12 and 24 hr) annual maximum rainfall depths measured by more than 5,000 rain gauges from 1916 up to 2023 all over Italy. In this work, rain gauges active in the 1931–2020 period located over the Po River basin are considered. An improved version of the patched kriging (Libertino et al., 2018; Mazzoglio et al., 2022; Paola Mazzoglio & Claps, 2023), a robust gap-filling procedure for

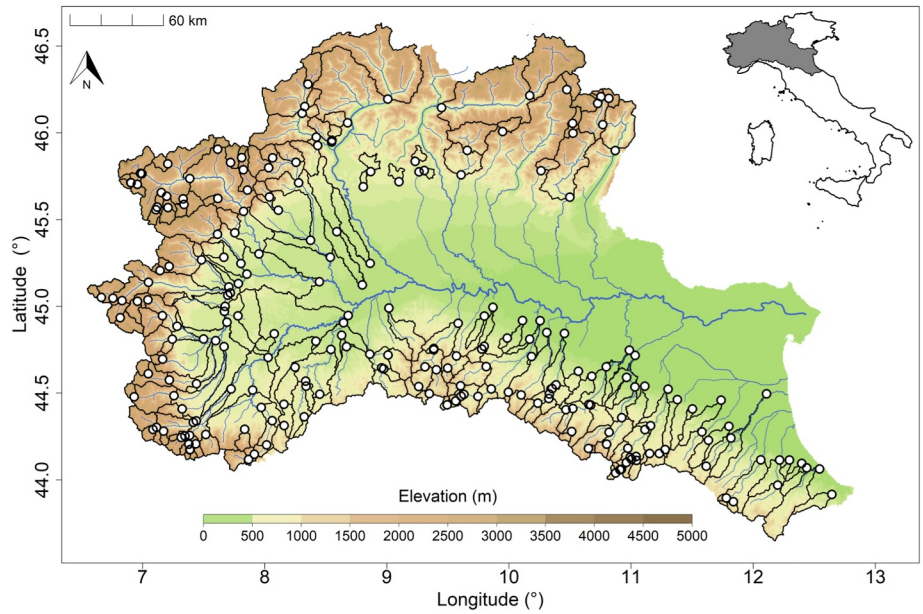

Figure 5. Location of the 227 analyzed sites and identification of the basin boundaries.

rainfall frequency analysis, was used to exploit all the available rainfall information. This methodology makes it possible to obtain an estimation of the IDF curve parameters for selected distributions (e.g., the Gumbel in our work) in gauged and ungauged locations. These curves follow Equation 12

$$h_{d,T} = K_T \cdot a \cdot d^n = \left[1 - 0.5772 \cdot \sigma - \sigma \cdot \ln\left(\ln\left(\frac{T}{T-1}\right)\right)\right] \cdot a \cdot d^n \tag{12}$$

where $h_{d,T}$ is the design rainfall related to duration d and return period T (mm); K_T is the growth factor related to a return period T, modeled as a Gumbel distribution with mean 1 and non-dimensional scale parameter σ (−); a is the scale factor (mm/hr), that is, the expected maximum annual 1-hr precipitation; d is the duration (h); and n is the scaling exponent (−) that describes the rate of increase of the expected maximum annual precipitation for increasing durations. The methodology consists of three main steps: (a) interpolation with a regression kriging of annual maximum rainfall depths performed year by year, separately for each duration, to obtain a rainfall data cube with a spatial extent matching the analysis areas and a number of layers equal to the number of years considered; (b) calculation of the L-moments of the reconstructed series (which may originate from direct measurements or kriging interpolation), with an approach that gives greater weight to measured values; (c) bias correction of both the L-moments and the reconstructed time series. The a and n parameters are estimated, respectively, as the intercept and the slope of the simple linear regression model applied to the logarithm of the mean rainfall extremes for 1, 3, 6, 12, and 24-hr durations. The growth factor parameter σ is estimated with the method of L-moments as $\frac{L_{cv}}{\ln(2)}$, where L_{cv} is the L-coefficient of variation of the annual maxima of precipitation with duration d. The value of K_T is assumed to be the same for all the duration of precipitation, and is estimated as the mean of the K_T obtained for the 5 durations. The reader can refer to Libertino et al. (2018) for a more detailed description of the patched kriging methodology and to Paola Mazzoglio and Claps (2023) for more details on the regression model implemented to perform the year-by-year reconstruction. The entire patched kriging workflow is here run during the period 1931–2020 to obtain the growth factor for the Gumbel distribution for return periods of 2, 5, 10, 20, 50, 100, 200, 500, and 1,000 years. For every catchment, we consider a time of concentration roughly estimated from its drainage area as $t_c = 0.675 \cdot A^{0.5}$ (Ferro, 2006). This formula is one of those used in Ravazzani et al. (2019) to estimate the time of concentration of 46 basins in northern Italy and was chosen for its simplicity (see Evangelista et al. (2023) for a review on catchment response time formulas). For the application of the q-q methodology, the evaluation

of the time of concentration is a key aspect when the growth factor is different for different durations. To analyze the expected variation of the IDF curves in the future, we use an ensemble of 24 simulations of CORDEX models (EUR-11) of CMIP5 (Jacob et al., 2014; Taylor et al., 2012) with a spatial resolution of 12.5 km, temporal resolution of 1h and RCP 8.5. We consider a control period (1981–2010) and a future period (2071–2100) calculating the percentage variation of precipitation quantiles with the same procedure previously described in Equation 11. Note that using percentage variation, no bias-correction procedure is needed. CORDEX models of CMIP5 were used because of the availability of a large number of different simulations over the study area (Appendix A). The percentage variation of precipitation quantiles considered in the case study is the median of those obtained from the single simulations.

4.2. Flood Frequency Curves of Discharge Extremes

For estimating the FFCs, we use the Spatially Smooth Estimation Method developed by Laio et al. (2011), which is one of the methods now operationally used in the area. This regionalization procedure is based on the definition of a set of three generalized least squares regression models that are suitable for the estimation of the L-moments of the distribution in ungauged catchments (Griffis & Stedinger, 2007). The regression equations use morpho-climatic descriptors as predictors to estimate the L-moments of the distribution. In particular, we estimate the mean $\left(q_{ind}\right)$, the coefficient of L-variation (L_{cv}) and the L-skewness (L_{ca}) of the record (Laio et al., 2011). Equation 13 reports the regressions obtained for the study area:

$$\begin{aligned} q_{\text{ind}} &= 0.01239 \cdot A^{0.77905} \cdot k_s^{-0.16514} \cdot a^{2.09555} \cdot n^{1.3146} \\ L_{\text{cv}} &= 0.30465 - 0.00013 \cdot MAP_{\text{mean}} - 0.12571 \cdot MAP_{\text{cv}} - 0.00541 \cdot C2 \\ L_{\text{ca}} &= -0.40728 - 0.2167 \cdot MAP_{\text{cv}} + 2.78896 \cdot L_{ca_{3\text{h}}} - 0.00366 \cdot C2 \end{aligned} \tag{13}$$

where A is the area of the catchment (km^2); k_s is the saturated permeability coefficient (−), calculated as in Claps et al. (2024); MAP_{mean} is the spatial average of the mean annual precipitation over the basin (mm); MAP_{cv} is the spatial coefficient of variation of the mean annual precipitation over the basin (−); $L_{ca_{3\text{h}}}$ is the spatial mean of the L-skewness of annual maximum rainfall for the duration of 3 hr (−); $C2$ is the mean value of the C2 coefficient in the Fourier series representation of the monthly rainfall regime (−) as explained in Claps et al. (2024). When data are available for the section of interest, they are integrated into the estimation to make it more robust by using the sample or regional L-moments based on their estimation variability (Laio et al., 2011). For each basin, the flood quantiles are assumed to follow a 3-parameters log-normal distribution, whose CDF is:

$$F_Q(z) = \Phi\left(\frac{\ln(z-\theta_1)-\theta_2}{\theta_3}\right) \tag{14}$$

where θ_1, θ_2 and θ_3 are obtained from the L-moments (Hosking & Wallis, 1997) and Φ is the normal CDF function.

4.3. Results of the Case Study

The basin data set was first analyzed in terms of catchment response and precipitation distribution parameters variation, identifying 22 basins that required special attention based on the results of the sensitivity analysis. In Appendix B, the procedure applied to subset the data set is described. These catchments exhibit characteristics that may result in a percentage error larger than 15% in the estimation of the 100-year flood. Figure 6 (panel c) shows the percentage changes in the 100-year flood for the study area, obtained with the proposed method based on the q-q relationship. The values range between 7% and 90%, but the large majority of the catchments are expected to face an increase of 20%–40%. The largest values are mostly found in smaller basins where the precipitation increase is more relevant: the smallest values are instead found in the Valle d'Aosta region in the north-western part of the study area. Most of the critical basins are high-elevation catchments in this area, where floods are often driven by snowmelt. The totality of the catchments included in the case study is expected to undergo an increase in the 100-year flood because, according to the CORDEX models, the precipitation with a

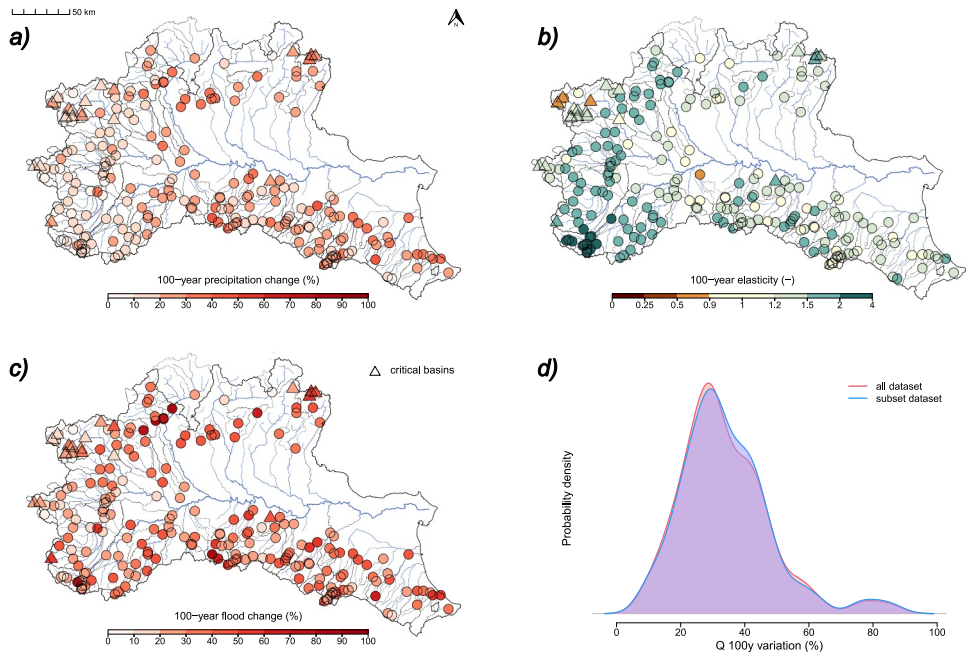

Figure 6. (a) Percentage change of the 100-year return period flood obtained for the period 2071–2100 versus 1981–2010 with the RCP8.5 scenario. (b) Percentage increase of the 100-year return period precipitation with duration equal to the time of concentration of the catchment considering the ensemble mean of the CORDEX models with the RCP8.5 scenario. (c) Elasticity for the 100-year return period based on the regional models applied for the flood and precipitation frequency curves. (d) Probability density function of the predicted variation of Q_{100} both for the subset data set and for the entire one.

return period of 100 years is expected to increase in all the study area. Results for two example catchments are also shown in Appendix C. The percentage increase of the flood quantiles results from the combination of two distinct factors: the first one is the increase of precipitation quantiles with a duration equal to the concentration time of the catchment, and the second is related to the elasticity of floods to precipitation E^{qq}. The percentage changes of Figure 6 (panel c) are obtained by the combination of these two factors (panels a and b). Some spatial patterns are found regarding the elasticity (E^{qq}_{100}) : the south-western part of the study area is characterized by the largest values with E^{qq}_{100} ranging between 2 and 2.5, while the north-western part has the lowest values with many basins with E^{qq}_{100} smaller than 1. Regarding the precipitation increase, there are some small basins with exceptional increases because they have small concentration times, and short precipitation extremes are projected to increase more than long ones. The clearest and more robust signal is instead found in the Emilia-Romagna region in the Apennine basins (south-western part of the map), where the increase approaches values of 30%. Figure 6 (panel d) shows the density function of the predicted variation of Q_{100} both for the subset data set and for the entire one. The exclusion of the 22 basins does not significantly alter the probability density of Q_{100} overall.

5. Discussion

In this work, we propose a method to include the expected variation of extreme precipitation into flood frequency analysis based on the assumption that the quantile-quantile relationship between precipitation and flood distributions is stationary. We asked three questions about the proposed methodology: (a) In which conditions are we allowed to use the methodology? (b) Is this methodology suitable for all the percentiles across the full distribution of floods? (c) What are the expected flood changes for projected precipitation changes in Northern Italy? Regarding the first question, we identify a range of cases in which this methodology can be applied. The target catchment for applying this methodology shows a medium to strong correlation between the annual maxima of rainfall and floods, indicating that extreme rainfall is the main flood generation mechanism. One approach to characterize a catchment in this context is to analyze the seasonality of floods and rainfall; if these differ, this may indicate that the q-q methodology has a limitation.

When data are available, we also suggest analyzing continuous series of precipitation and discharge, isolating some events following, for example, Tarasova et al. (2018) or Giani et al. (2022), and examining the correlation between precipitation and runoff coefficient at the event scale. Moreover, the response type of the catchment in terms of rainfall-runoff transformation was found to be a fundamental aspect to consider. Errors are larger in catchments with generally low values of the peak runoff coefficient of the annual flood, that is, arid catchments or high-infiltration catchments. Another factor to consider before employing this methodology is the variation of rainfall distribution. When the distribution is expected to change more in terms of the variance rather than the mean, larger errors may occur in the estimation of future flood quantiles. While each of these aspects has to be considered, we believe the methodology should be discarded only when the catchment presents criticalities in all of them, as PE larger than 15% occurred only in such cases.

Concerning the second question, the q-q approach is recommended for large values of return periods ($T > 100$ years), for which our results show that the percentage error of future flood quantiles remains small. Note that the estimation of precipitation and flood quantiles, as well as their variations, are subject to larger uncertainty for high return periods, but the proposed methodology is more reliable. For this reason, we suggest using FFCs and IDF curves obtained through regional methods, which are more robust in capturing the tail behavior of the distributions than methods applied locally on data belonging to single sites. Additionally, for large return periods, the q-q curve is less influenced by changes in the runoff coefficient parameters, which in this validation analysis were kept constant given that we are only interested in the effect of the variation of rainfall. This is because the effect of a change in the runoff generation processes is more likely to have an influence on the lower part of the q-q relationship, describing ordinary floods that can be produced by large rainfall and moderate runoff coefficient or the other way around, while for larger return periods, when initial conditions of the catchment become less relevant under the assumption that big floods are always caused by large rainfall and runoff coefficient, the q-q relationship is less sensitive to changes in their distribution. This interpretation is consistent with Macdonald et al. (2024), who analyzed the tail behavior of flood and precipitation distributions. They found that beyond a certain return period, the influence of catchment processes decreases, and the tail of rainfall distribution modulates the tail of flood peak distribution. The threshold value of the return period depends on the ratio between catchment storage and mean annual rainfall. Most of the catchments they analyzed have a threshold return period between 100 and 500 years. Brunner et al. (2021) related instead the threshold return period with mean catchment elevation finding that for high-elevation catchment this value drops below 10 years. This implies that the return periods for which our methodology may be considered more accurate vary depending on the catchment of interest.

Analyzing the results of the case study, two distinct factors causing changes in flood quantiles are found. The first one is the percentage increase of the corresponding precipitation quantiles, while the second one is the elasticity of floods to precipitation changes. Large values of elasticity are found in catchments with particularly steep FFCs compared to the IDF curves. In these catchments, even a small increase of precipitation quantiles can produce a large increase in flood quantiles (e.g., a catchment with $E = 2$ will face a 40% increase of flood quantile as a result of a 20% increase of the precipitation quantile increase). Note that an elasticity of 2 has been found by Haslinger et al. (2025) between heavy hourly rainfall and flood peak increase in small basins in Austria, which is consistent with the range of elasticities we estimate through the qq relationship in Northern Italy. Here, some spatial patterns can be identified: the south-western part of the study area, which is characterized by steep FFC (i.e., large values of L-skewness), has the largest values. The lowest values are instead found in north-western part of the study area, where snow processes are dominant given the very high elevations. Regarding the first one, a possible interpretation is given by the role of geology. In this region, springs are fed by aquifers hosted in highly fractured carbonate successions. The carbonate rock mass is bordered by the impermeable metamorphic bedrock, which in general constitutes important permeability sills. This area is also characterized by a fractured and karstic aquifer with an extensive saturated zone, or karst carbonate aquifer covered by a thick layer of glacial deposits that heavily control the infiltration processes (Vigna & Banzato, 2015). These characteristics result in large infiltration during small events, while the karst system has a relevant contribution during major events. With reference to the rational method, this results in particularly low values of C and, consequently, in large values of elasticity. Regarding the north-western part of the study area, floods often result from snowmelt, leading to less variable mechanisms that produce a flatter FFC and lower elasticity values ($E_{100} < 1$). Breinl et al. (2021) similarly

observed inelastic relationships in the glaciated regions of the highest summits of Austria. Most of the basins in question are among those identified as potentially critical in the analysis described in Appendix B. When analyzing snow-dominated catchments, a more rigorous approach would involve removing the base flow and isolating floods generated by large precipitation events before applying the proposed methodology.

The results of the increase of the 100-year floods obtained with our methodology agree with those obtained in other studies that used different methodologies. For example, Rojas et al. (2012) assessed future flood hazard in view of climate change at a pan-European scale using a large ensemble of climate projections. They used hydrological models forced by bias-corrected climate data from an ensemble of 12 climate experiments conducted within the ENSEMBLES project, obtaining spatial patterns of variation of the 100-year flood in Europe. In particular, northern Italy shows a robust increase (about 40% when comparing the period 2071–2100 and 1961–1990), mainly due to a pronounced increase in extreme rainfall. A similar approach was used by Roudier et al. (2016) who presented an assessment of the impacts of a +2°C global warming on extreme floods, obtaining an increase of Q_{100} in northern Italy between 30% and 40%. Similar values of Q_{100} increase in Northern Italy were also found by Kundzewicz et al. (2010), who reviewed projections of flood hazard in Europe based on climatic and hydrological models, to illustrate possible changes of recurrence of a 100-year flood in Europe. Signals of increase in magnitude of the 100-year floods in Northern Italy were also found by Di Sante et al. (2021), who simulated climate change effects on the occurrence of river floods over Europe. They used a distributed hydrological model (CHyM) forced with 44 EURO-CORDEX, 13 CMIP5, and 7 CMIP6 simulations finding a robust signal of flood magnitude increase due to the increase of extreme precipitation events. Compared to these approaches, the advantage of the q-q methodology is that complex rainfall-runoff modeling is avoided.

6. Conclusions

In this work, we develop an approach that can be used for flood frequency analysis including the effect of the predicted change in precipitation extremes, also in ungauged basins. The method is based on a combination of a data-based approach to obtain the q-q relationships for each catchment and a model-based approach to obtain the expected variation of the IDF curves. It allows to modify regional FFC accounting for the expected variation of regional IDF curves according to climate models. The methodology constitutes a simple but effective tool for decision-makers, which can be used over many catchments in a wide area, such as the one investigated in this work (coincident with the largest Italian water district). The results obtained in the case study presented here are comparable with those found in other studies that used more complex approaches to evaluate the percentage change of the 100-year flood. This methodology should be applied when the expected flood change is dominated by changes in rainfall extremes rather than in the runoff generation processes of the catchment. In addition, it is expected to provide more reliable results for large return periods and for catchments characterized by a medium-to-large correlation between flood and rainfall annual maxima. This study can be considered as an example of "flood frequency hydrology," in a broader sense of what is discussed in Merz and Blöschl (2008a), Merz and Blöschl (2008b), and Viglione et al. (2013), that is, a way of expanding information on how climate change may affect floods by using different techniques and data in a different way that is usually done in studies of non-stationarity on floods. Future research should further test and refine this approach, but our findings suggest that the q-q relationship, and particularly its elasticity, can serve as a practical tool for incorporating extreme precipitation variations into flood frequency analysis, ultimately allowing flood risk assessment under climate change.

Appendix A

Table A1 shows the list of the CORDEX simulations used to evaluate the expected variation of the Intensity-Duration-Frequency curves.

Table A1
List of CORDEX Simulations Included in the Ensemble Mean Used to Evaluate the Expected Variation of the Intensity-Duration-Frequency Curves

GCM name	RCM name
MPI-ESM-LR	GERICS-REMO2015
MPI-ESM-LR	CLMcom-ETH-COSMO-crCLIM-v1-1
MPI-ESM-LR	CNRM-ALADIN63
MPI-ESM-LR	MOHC-HadREM3-GA7-05
NCC-NorESM1-M	SMHI-RCA4
NCC-NorESM1-M	CLMcom-ETH-COSMO-crCLIM-v1-1
NCC-NorESM1-M	CNRM-ALADIN63
NCC-NorESM1-M	MOHC-HadREM3-GA7-05
NCC-NorESM1-M	ICTP-RegCM4-6
CNRM-CERFACS-CNRM-CM5	SMHI-RCA4
CNRM-CERFACS-CNRM-CM5	CNRM-ALADIN63
CNRM-CERFACS-CNRM-CM5	GERICS-REMO2015
CNRM-CERFACS-CNRM-CM5	ICTP-RegCM4-6
CNRM-CERFACS-CNRM-CM5	MOHC-HadREM3-GA7-05
CNRM-CERFACS-CNRM-CM5	CLMcom-ETH-COSMO-crCLIM-v1-1
IPSL-IPSL-CM5A-MR	SMHI-RCA4
MOHC-HadGEM2-ES	SMHI-RCA4
MOHC-HadGEM2-ES	CLMcom-ETH-COSMO-crCLIM-v1-1
MOHC-HadGEM2-ES	MOHC-HadREM3-GA7-05
MOHC-HadGEM2-ES	SMHI-RCA4
ICHEC-EC-EARTH	CLMcom-ETH-COSMO-crCLIM-v1-1
ICHEC-EC-EARTH	ICTP-RegCM4-6
ICHEC-EC-EARTH	MOHC-HadREM3-GA7-05
ICHEC-EC-EARTH	SMHI-RCA4

Note. The models belong to the Fifth Assessment Report (AR5) of the IPCC and have a spatial resolution of 12.5 km.

Appendix B

In this section, additional information on the catchments characteristics of the case study are presented and put in relation with the sensitivity analysis, explaining how the list of potentially critical basins was obtained. Figure B1 shows the density probability of the location and scale parameters of the precipitation distribution, as well as their percentage variation between the periods 2071–2100 and 1981–2010. The values of the parameters used in the sensitivity analysis represent a typical small-to-medium Alpine catchment with an area ranging from 50 to 200 km^2. These values maximize the representativeness of the catchments analyzed in the case study. In our case study, the shape parameter ξ ranges between 30 and 50 mm for more than half of the catchments, with an increase from the present to the future period of less than 30% for almost the totality of the catchments. The scale parameter σ is between 10 and 15 mm for almost half of the catchments, with an increase of less than 60% for almost the totality of them. Similarly, we analyzed the catchments in terms of the ratio between the mean annual flood and the mean annual maximum precipitation as a proxy of the mean value of C (Figure B2). The 22 catchments selected as critical were those with a location increase larger than 20% and a value of $\frac{q_{\text{ind}}}{a \cdot d^{n-1}} < 0.2$. These catchments present characteristics that, according to the sensitivity analysis, may undergo a percentage error PE in the estimation of the 100-year flood larger than 15%. The catchments selected as potentially critical are not necessarily unsuitable for the analysis: the data available for the region does not allow us to gain information on the copula parameter θ, therefore, we chose to consider the worst-case scenario with $\theta = 1$, that is, no correlation between precipitation and runoff coefficient.

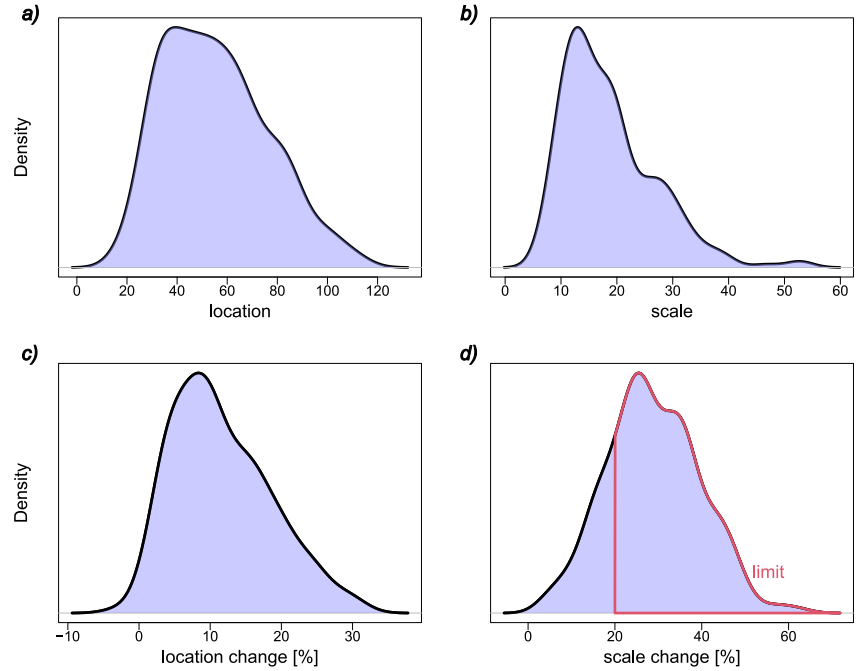

Figure B1. Density probability of the location and scale parameters of the precipitation distribution with duration equal to the time of concentration of the specific catchment (panels a and b). Percentage variation of the parameters when comparing the periods 2071–2100 and 1981–2010 (panels c and d). The range of values considered potentially critical is highlighted in red in panel (d).

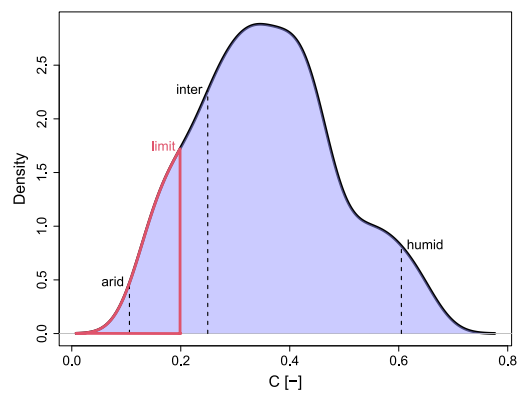

Figure B2. Density probability of the mean value of peak runoff coefficient, estimated as the ratio between index flood and index precipitation. The values corresponding to the arid, intermediate, and humid configurations described in the sensitivity analysis are highlighted, as well as the range of values considered potentially critical.

Appendix C

The results obtained for two example catchments are also reported. The "Dora Baltea at Ponte di Mombardone" is among the catchments with the lowest values of elasticity ($E_{100} = 0.8$), while the "Maira at San Damiano Macra" is among the most elastic catchments ($E_{100} = 2.3$). Forcing the quantile-quantile relationship to be stationary in time, it is possible to obtain in Figures C1 and C2 the expected variation of FFCs caused by a variation of the IDF curves. As we found in Section 3, the hypothesis of stationarity of the q-q relationship is credible for large return periods (100 years). In the second catchment, floods are more sensitive to an increase in precipitation intensity, and the percentage increase of Q_{100} is more than double the percentage increase of P_{100}.

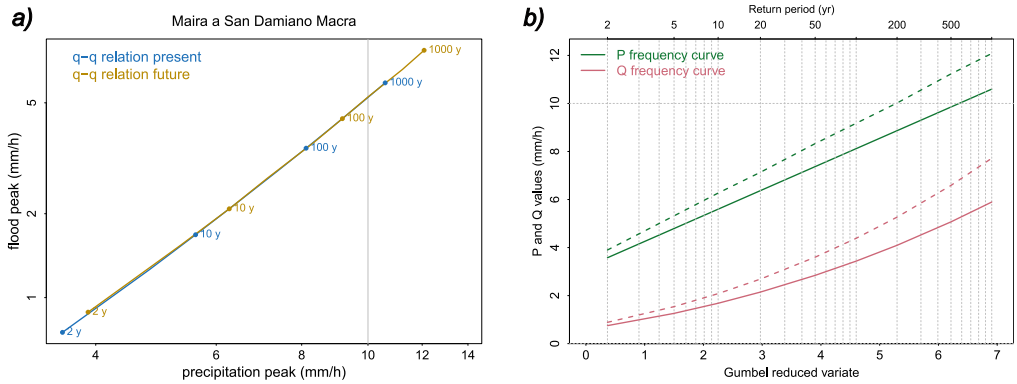

Figure C1. (a) q-q relationship obtained for the catchment "Dora Baltea at Ponte di Mombardone". The q-q relationships for the present and future periods are forced to coincide following the methodology described in the paper so that it is possible to obtain the future flood frequency curve considering the variation of the precipitation frequency curve. This catchment is characterized by a particularly small value of elasticity. In panel (b), the frequency curves of precipitation and flood are shown for the 1981–2010 (solid line) and the 2071–2100 periods (dashed line). Regarding the future frequency curves, the precipitation one is obtained through the ensemble mean of CORDEX models, while the flood one is obtained by forcing the quantile-quantile relationship to be stationary in time. The percentage variation of Q_{100} is smaller than the percentage variation of P_{100}.

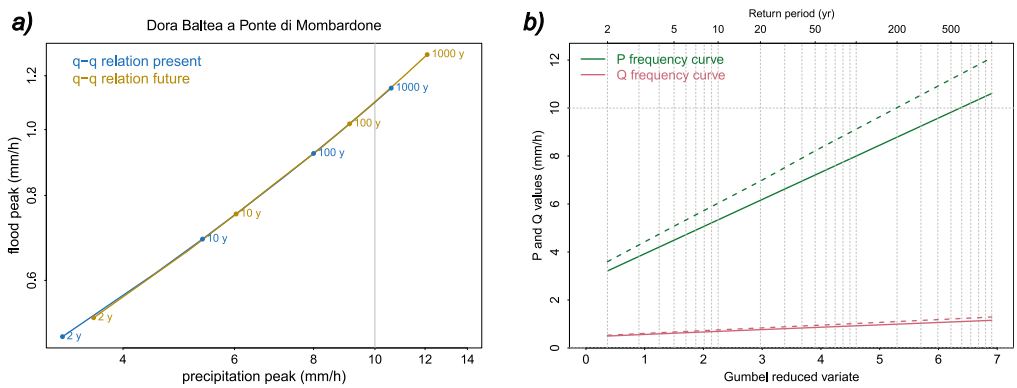

Figure C2. (a) q-q relationship obtained for the catchment "Maira at San Damiano Macra". The q-q relationships for the present and future periods are forced to coincide following the methodology described in the paper so that it is possible to obtain the future flood frequency curve considering the variation of the precipitation frequency curve. This catchment is characterized by a particularly large value of elasticity. In panel (b), the frequency curves of precipitation and flood are shown for the 1981–2010 (solid line) and the 2071–2100 periods (dashed line). Regarding the future frequency curves, the precipitation one is obtained through the ensemble mean of CORDEX models, while the flood one is obtained by forcing the quantile-quantile relationship to be stationary in time. The percentage variation of Q_{100} is larger than the percentage variation of P_{100}.

Acronyms

FFC	flood frequency curve
IDF	intensity-duration-frequency curve
E	elasticity
PE	percentage error

Notation

Q	flood peak [mm/hr] random variable (a particular value is indicated by z)
q_Q	flood peak quantile with probability level p [mm/hr]
t_c	critical storm duration (time of concentration) [hr]
C	runoff coefficient [–] random variable (a particular value is indicated by x)
P	precipitation intensity for the critical storm duration [mm/hr] random variable (a particular value is indicated by y)
q_P	precipitation intensity quantile with probability level p [mm/hr]
τ_k	Kendall tau
θ	Gumbel copula parameter
q_{ind}	L-moment of order one (the mean) [mm/hr]
L_{cv}	coefficient of L-variation [–]
L_{ca}	L-skewness [–]
k_s	saturated permeability coefficient [–]
MAP_{mean}	the spatial average of the mean annual precipitation over the basin [mm]
MAP_{cv}	spatial coefficient of variation of the mean annual precipitation over the basin [–]
$L_{ca_{3h}}$	spatial mean of the L-skewness of annual maximum rainfall for the duration of 3 hr [–]
$C2$	The mean value of the $C2$ coefficient in the Fourier series representation of the rainfall regime [–]
$\theta_1, \theta_2, \theta_3$	log-normal distribution parameters [–]
ξ, σ	Gumbel distribution parameters [–]
α, β	Beta distribution parameters [–]
$f_X(.)$	probability density function of X
$F_X(x\|y)(.)$	conditional cumulative distribution function of x given y
$F_x(.)$	cumulative distribution function of X
$f^{-1}(.)$	inverse function of f
$\Phi(.)$	cumulative function of normal distribution

Data Availability Statement

The data analysis was performed using R Core Team (2021). The R scripts and the data used to execute the analyses in the paper can be found at Cafiero (2025).

Acknowledgments
This study was carried out within the RETURN Extended Partnership and received funding from the European Union Next-GenerationEU (National Recovery and Resilience Plan—NRRP, Mission 4, Component 2, Investment 1.3—D.D. 1243 2/8/2022, PE0000005) and from the Italian Ministry of University and Research (PRIN project n. 2022AX3882 - Clim2FlEx - Mapping of climate to flood extremes).

References

Anzolin, G., Chaffe, P. L. B., Vrugt, J. A., & AghaKouchak, A. (2023). Using climate information as covariates to improve nonstationary flood frequency analysis in Brazil. *Hydrological Sciences Journal*, *68*(5), 645–654. https://doi.org/10.1080/02626667.2023.2182212

Barbhuiya, S., Ramadas, M., & Biswal, S. S. (2023). Nonstationary flood frequency analysis: Review of methods and models. In M. Pandey, A. K. Gupta, & G. Oliveto (Eds.), *River, sediment and hydrological extremes: Causes, impacts and management* (pp. 271–288). Springer Nature Singapore. https://doi.org/10.1007/978-981-99-4811-6_15

Bertola, M., Viglione, A., Lun, D., Hall, J., & Blöschl, G. (2020). Flood trends in Europe: Are changes in small and big floods different? *Hydrology and Earth System Sciences*, *24*(4), 1805–1822. https://doi.org/10.5194/hess-24-1805-2020

Bertola, M., Viglione, A., Vorogushyn, S., Lun, D., Merz, B., & Blöschl, G. (2021). Do small and large floods have the same drivers of change? A regional attribution analysis in Europe. *Hydrology and Earth System Sciences*, *25*(3), 1347–1364. https://doi.org/10.5194/hess-25-1347-2021

Bloetscher, F. (2012). Protecting people, infrastructure, economies, and ecosystem assets: Water management in the face of climate change. *Water*, *4*(2), 367–388. https://doi.org/10.3390/w4020367

Blöschl, G., Ardoin-Bardin, S., Bonell, M., Dorninger, M., Goodrich, D., Gutknecht, D., et al. (2007). At what scales do climate variability and land cover change impact on flooding and low flows? *Hydrological Processes*, *21*(9), 1241–1247. https://doi.org/10.1002/hyp.6669

Blöschl, G., Buttinger-Kreuzhuber, A., Cornel, D., Eisl, J., Hofer, M., Hollaus, M., et al. (2024). Hyper-resolution flood hazard mapping at the national scale. *Natural Hazards and Earth System Sciences*, *24*(6), 2071–2091. https://doi.org/10.5194/nhess-24-2071-2024

Breinl, K., Lun, D., Müller-Thomy, H., & Blöschl, G. (2021). Understanding the relationship between rainfall and flood probabilities through combined intensity-duration-frequency analysis. *Journal of Hydrology*, *602*, 126759. https://doi.org/10.1016/j.jhydrol.2021.126759

Brunner, M. I., Swain, D. L., Wood, R. R., Willkofer, F., Done, J. M., Gilleland, E., & Ludwig, R. (2021). An extremeness threshold determines the regional response of floods to changes in rainfall extremes. *Communications Earth and Environment*, *2*(1), 173. https://doi.org/10.1038/s43247-021-00248-x

Cafiero, L. (2025). How changes in future precipitation impact flood frequencies: A quantile-quantile mapping approach [Dataset]. *Zenodo*. https://doi.org/10.5281/zenodo.15544579

Claps, P., Evangelista, G., Ganora, D., Mazzoglio, P., & Monforte, I. (2024). FOCA: A new quality-controlled database of floods and catchment descriptors in Italy. *Earth System Science Data*, *16*(3), 1503–1522. https://doi.org/10.5194/essd-16-1503-2024

Cunderlik, J. M., & Burn, D. H. (2003). Non-stationary pooled flood frequency analysis. *Journal of Hydrology*, *276*(1), 210–223. https://doi.org/10.1016/S0022-1694(03)00062-3

Di Sante, F., Coppola, E., & Giorgi, F. (2021). Projections of river floods in Europe using EURO-CORDEX, CMIP5 and CMIP6 simulations. *International Journal of Climatology*, *41*(5), 3203–3221. https://doi.org/10.1002/joc.7014

Dong, X., Jiang, L., Zeng, S., Guo, R., & Zeng, Y. (2020). Vulnerability of urban water infrastructures to climate change at city level. *Resources, Conservation and Recycling*, *161*, 104918. https://doi.org/10.1016/j.resconrec.2020.104918

European Commission, D.-G. F. E. (2021). *Impact of climate change on floods: Survey findings and possible next steps to close the knowledge and implementation gap – Final a survey based study*. Publications Office. https://doi.org/10.2779/932572

Evangelista, G., Woods, R., & Claps, P. (2023). Dimensional analysis of literature formulas to estimate the characteristic flood response time in ungauged basins: A velocity-based approach. *Journal of Hydrology*, *627*, 130409. https://doi.org/10.1016/j.jhydrol.2023.130409

Ferro, V. (2006). Riqualificazione ambientale dei corsi d'acqua. *Quaderni di Idronomia Montana*, *25*, 1–20.

Fiorentino, M., Manfreda, S., & Iacobellis, V. (2007). Peak runoff contributing area as hydrological signature of the probability distribution of floods. *Advances in Water Resources*, *30*(10), 2123–2134. https://doi.org/10.1016/j.advwatres.2006.11.017

Fiseha, B., Setegn, S., Melesse, A., Volpi, E., & Fiori, A. (2014). Impact of climate change on the hydrology of upper Tiber River Basin using bias corrected regional climate model. *Water Resources Management: An International Journal, Published for the European Water Resources Association (EWRA)*, *28*(5), 1327–1343. https://doi.org/10.1007/s11269-014-0546-x

Giani, G., Tarasova, L., Woods, R. A., & Rico-Ramirez, M. A. (2022). An objective time-series-analysis method for rainfall-runoff event identification. *Water Resources Research*, *58*(2), e2021WR031283. https://doi.org/10.1029/2021WR031283

Gobiet, A., Kotlarski, S., Beniston, M., Heinrich, G., Rajczak, J., & Stoffel, M. (2014). 21st century climate change in the European Alps—A review. *Science of the Total Environment*, *493*, 1138–1151. https://doi.org/10.1016/j.scitotenv.2013.07.050

Gottschalk, L., & Weingartner, R. (1998). Distribution of peak flow derived from a distribution of rainfall volume and runoff coefficient, and a unit hydrograph. *Journal of Hydrology*, *208*(3–4), 148–162. https://doi.org/10.1016/s0022-1694(98)00152-8

Griffis, V., & Stedinger, J. (2007). The use of GLS regression in regional hydrologic analyses. *Journal of Hydrology*, *344*(1), 82–95. https://doi.org/10.1016/j.jhydrol.2007.06.023

Guo, S., Xiong, L., Chen, J., Guo, S., Xia, J., Zeng, L., & Xu, C.-Y. (2022). Nonstationary regional flood frequency analysis based on the Bayesian method. *Water Resources Management*, *37*(2), 1–23. https://doi.org/10.1007/s11269-022-03394-9

Hall, J., Arheimer, B., Borga, M., Brázdil, R., Claps, P., Kiss, A., et al. (2014). Understanding flood regime changes in Europe: A state-of-the-art assessment. *Hydrology and Earth System Sciences*, *18*(7), 2735–2772. https://doi.org/10.5194/hess-18-2735-2014

Haslinger, K., Breinl, K., Pavlin, L., Pistotnik, G., Bertola, M., Olefs, M., et al. (2025). Increasing hourly heavy rainfall in Austria reflected in flood changes. *Nature*, *639*(8055), 667–672. https://doi.org/10.1038/s41586-025-08647-2

Hosking, J. R. M., & Wallis, J. R. (1997). L-moments. In *Regional frequency analysis: An approach based on L-moments* (pp. 14–43). Cambridge University Press. https://doi.org/10.1017/CBO9780511529443.004

Jacob, D., Petersen, J., Eggert, B., Alias, A., Christensen, O., Bouwer, L., et al. (2014). EURO-CORDEX: New high-resolution climate change projections for European impact research. *Regional Environmental Change*, *14*(2), 563–578. https://doi.org/10.1007/s10113-013-0499-2

Koutsoyiannis, D., & Montanari, A. (2015). Negligent killing of scientific concepts: The stationarity case. *Hydrological Sciences Journal*, *60*(7–8), 1174–1183. https://doi.org/10.1080/02626667.2014.959959

Kundzewicz, Z., Lugeri, N., Dankers, R., Hirabayashi, Y., Döll, P., Pińskwar, I., et al. (2010). Assessing river flood risk and adaptation in Europe—Review of projections for the future. *Climate Change*, *15*(7), 641–656. https://doi.org/10.1007/s10584-015-1570-4

Laio, F., Ganora, D., Claps, P., & Galeati, G. (2011). Spatially smooth regional estimation of the flood frequency curve (with uncertainty). *Journal of Hydrology*, *408*(1), 67–77. https://doi.org/10.1016/j.jhydrol.2011.07.022

Leclerc, M., & Ouarda, T. B. (2007). Non-stationary regional flood frequency analysis at ungauged sites. *Journal of Hydrology*, *343*(3), 254–265. https://doi.org/10.1016/j.jhydrol.2007.06.021

Libertino, A., Allamano, P., Laio, F., & Claps, P. (2018). Regional-scale analysis of extreme precipitation from short and fragmented records. *Advances in Water Resources*, *112*, 147–159. https://doi.org/10.1016/j.advwatres.2017.12.015

Macdonald, E., Merz, B., Guse, B., Nguyen, V. D., Guan, X., & Vorogushyn, S. (2024). What controls the tail behaviour of flood series: Rainfall or runoff generation? *Hydrology and Earth System Sciences*, *28*(4), 833–850. https://doi.org/10.5194/hess-28-833-2024

Mangini, W., Viglione, A., Hall, J., Hundecha, Y., Ceola, S., Montanari, A., et al. (2018). Detection of trends in magnitude and frequency of flood peaks across Europe. *Hydrological Sciences Journal*, *63*(4), 493–512. https://doi.org/10.1080/02626667.2018.1444766

Mazzoglio, P., Butera, I., Alvioli, M., & Claps, P. (2022). The role of morphology in the spatial distribution of short-duration rainfall extremes in Italy. *Hydrology and Earth System Sciences*, *26*(6), 1659–1672. https://doi.org/10.5194/hess-26-1659-2022

Mazzoglio, P., Butera, I., & Claps, P. (2020). I^2-RED: A massive update and quality control of the Italian annual extreme rainfall dataset. *Water*, *12*(12), 3308. https://doi.org/10.3390/w12123308

Merz, R., & Blöschl, G. (2008a). Flood frequency hydrology: 1. Temporal, spatial, and causal expansion of information. *Water Resources Research*, *44*(8), W08432. https://doi.org/10.1029/2007WR006744

Merz, R., & Blöschl, G. (2008b). Flood frequency hydrology: 2. Combining data evidence. *Water Resources Research*, *44*(8), W08433. https://doi.org/10.1029/2007WR006745

Merz, R., Blöschl, G., & Parajka, J. (2006). Spatio-temporal variability of event runoff coefficients. *Journal of Hydrology*, *331*(3–4), 591–604. https://doi.org/10.1016/j.jhydrol.2006.06.008

Mishra, B. K., & Herath, S. (2015). Assessment of future floods in the Bagmati River Basin of Nepal using bias-corrected daily GCM precipitation data. *Journal of Hydrologic Engineering*, *20*(8), 05014027. https://doi.org/10.1061/(ASCE)HE.1943-5584.0001090

Mulvaney, T. (1850). On the use of self-registering rain and flood gauges. *Proceedings-Institution of Civil Engineers*, *4*, 1–8.

Paola Mazzoglio, I. B., & Claps, P. (2023). A local regression approach to analyze the orographic effect on the spatial variability of sub-daily rainfall annual maxima. *Geomatics, Natural Hazards and Risk*, *14*(1), 2205000. https://doi.org/10.1080/19475705.2023.2205000

Ravazzani, G., Boscarello, L., Cislaghi, A., & Mancini, M. (2019). Review of time-of-concentration equations and a new proposal in Italy. *Journal of Hydrologic Engineering*, *24*(10), 04019039. https://doi.org/10.1061/(ASCE)HE.1943-5584.0001818

R Core Team. (2021). R: A language and environment for statistical computing [Computer software manual]. *R Foundation*. Retrieved from https://www.R-project.org/

Rojas, R., Feyen, L., Bianchi, A., & Dosio, A. (2012). Assessment of future flood hazard in Europe using a large ensemble of bias-corrected regional climate simulations. *Journal of Geophysical Research*, *117*(D17), D17109. https://doi.org/10.1029/2012JD017461

Roudier, P., Andersson, C., Donnelly, J., Feyen, L., Greuell, W., & Ludwig, F. (2016). Projections of future floods and hydrological droughts in Europe under a +2°C global warming. *Climate Change*, *135*(2), 341–355. https://doi.org/10.1007/s10584-015-1570-4

Šraj, M., Viglione, A., Parajka, J., & Blöschl, G. (2016). The influence of non-stationarity in extreme hydrological events on flood frequency estimation. *Journal of Hydrology and Hydromechanics*, *64*(4), 426–437. https://doi.org/10.1515/johh-2016-0032

Steirou, E., Gerlitz, L., Apel, H., Sun, X., & Merz, B. (2019). Climate influences on flood probabilities across Europe. *Hydrology and Earth System Sciences*, *23*(3), 1305–1322. https://doi.org/10.5194/hess-23-1305-2019

Tarasova, L., Basso, S., Zink, M., & Merz, R. (2018). Exploring controls on rainfall-runoff events: 1. Time series-based event separation and temporal dynamics of event runoff response in Germany. *Water Resources Research*, *54*(10), 7711–7732. https://doi.org/10.1029/2018WR022587

Taylor, K. E., Stouffer, R. J., & Meehl, G. A. (2012). An overview of CMIP5 and the experiment design. *Bulletin of the American Meteorological Society*, *93*(4), 485–498. https://doi.org/10.1175/BAMS-D-11-00094.1

Viglione, A., Merz, B., Viet Dung, N., Parajka, J., Nester, T., & Blöschl, G. (2016). Attribution of regional flood changes based on scaling fingerprints. *Water Resources Research*, *52*(7), 5322–5340. https://doi.org/10.1002/2016WR019036

Viglione, A., Merz, R., & Blöschl, G. (2009). On the role of the runoff coefficient in the mapping of rainfall to flood return periods. *Hydrology and Earth System Sciences*, *13*(5), 577–593. https://doi.org/10.5194/hess-13-577-2009

Viglione, A., Merz, R., Salinas, J. L., & Blöschl, G. (2013). Flood frequency hydrology: 3. A Bayesian analysis. *Water Resources Research*, *49*(2), 675–692. https://doi.org/10.1029/2011WR010782

Vigna, B., & Banzato, C. (2015). The hydrogeology of high-mountain carbonate areas: An example of some Alpine systems in southern Piedmont (Italy). *Environmental Earth Sciences*, *74*(1), 267–280. https://doi.org/10.1007/s12665-015-4308-8

Villarini, G., Smith, J. A., Serinaldi, F., & Ntelekos, A. A. (2011). Analyses of seasonal and annual maximum daily discharge records for central Europe. *Journal of Hydrology*, *399*(3), 299–312. https://doi.org/10.1016/j.jhydrol.2011.01.007

Vogel, R. M., Yaindl, C., & Walter, M. (2011). Nonstationarity: Flood magnification and recurrence reduction factors in the United States. *JAWRA Journal of the American Water Resources Association*, *47*(3), 464–474. https://doi.org/10.1111/j.1752-1688.2011.00541.x

Westra, S., Alexander, L. V., & Zwiers, F. W. (2013). Global increasing trends in annual maximum daily precipitation. *Journal of Climate*, *26*(11), 3904–3918. https://doi.org/10.1175/JCLI-D-12-00502.1

Wilhelm, B., Rapuc, W., Amann, B., Anselmetti, F., Arnaud, F., Blanchet, J., et al. (2022). Impact of warmer climate periods on flood hazard in the European Alps. *Nature Geoscience*, *15*(2), 118–123. https://doi.org/10.1038/s41561-021-00878-y